Cervical and coelomic radiologic features of the loggerhead sea turtle, *Caretta caretta*

Ana Luisa Valente, Rafaela Cuenca, Maria Luz Parga, Santiago Lavín, Jordi Franch, Ignasi Marco

Abstract

Many investigators have undertaken radiologic studies in chelonians. However, descriptive papers focusing on the radiographic anatomy are limited to only a few species. The purpose of this article is to provide the normal cervical and coelomic radiographic appearance of the loggerhead sea turtle (*Caretta caretta*), in the dorsoventral view, and to indicate useful landmarks to identify internal anatomic structures. Dorsoventral radiographs were taken of the neck and body of 30 loggerhead sea turtles by means of analog and digital radiography. At various points, distortion or superimposition of images due to the natural curvature of the shell hindered the accuracy of interpretation. The pectoral and pelvic girdles were easily recognized. Important external landmarks included the vertebral and lateral scutes, and important internal landmarks included the bronchi, coracoid bones, the caudal border of the pulmonary fields, and the acetabulum.

Résumé

*Plusieurs chercheurs ont entrepris des études radiologiques chez les chéloniens. Toutefois, les articles descriptifs portant sur l'anatomie radiographique sont limités à seulement quelques espèces. Le but du présent article est de fournir l'apparence radiographique cervicale et coelomique normale, en vue dorso-ventrale, de la caouanne (*Caretta caretta*) et d'indiquer les repères utiles pour identifier les structures anatomiques internes. Des radiographies dorso-ventrales du cou et du corps de 30 caouannes ont été prises à l'aide de radiographies analogiques et digitales. À certains endroits, une distorsion ou une superposition des images causée par la courbure naturelle de la carapace interféra avec la précision de l'interprétation. Les gaines pectorale et pelvienne étaient facilement reconnaissables. Les repères externes importants incluaient les scutelles vertébrale et latérale, et les repères internes importants incluaient les bronches, les os coracoïdes, le bord caudal des champs pulmonaires et l'acétabulum.*

(Traduit par Docteur Serge Messier)

Introduction

Reptilian species often show the same nonspecific symptoms with a variety of diseases. Radiologic studies in chelonians have been described by many authors (1–7). However, owing to the great variability of species, papers dealing with radiographic anatomy are limited to a representative number of species of each order of *Reptilia* (8). In sea turtles, traumatic injuries of the shell and the ingestion of fishhooks are the most frequent causes of admission to marine-animal rescue centers (9). In most cases, physical examination does not give sufficient information, and dorsoventral radiography is usually the 1st option as an ancillary test to determine the diagnosis (10). Radiography gives a good overview of the skeletal system and in sea turtles is the most inexpensive and noninvasive method to detect ingested fishhooks and fractures (7). Nevertheless, as with many chelonian species, the image is often compromised by the overlying shell, which makes accurate interpretation difficult if the standard radiographic features are not well known. Detailed radiographic studies focusing on endangered sea turtles, such as the loggerhead (*Caretta caretta*), have not been available in the scientific literature and are needed as reference material for aquariums and marine-animal rescue centers.

In medicine, anatomic landmarks are used to indicate the location of biologic features (11). True landmarks are placed according to a biologic hypothesis of equivalence, or homology; pseudo-landmarks are placed on a surface according to a mathematical rule, such as a series of points distributed evenly along a given surface (12). The palpable external anatomic landmarks usually employed in veterinary medicine, such as the xyphoid tip, costal arch, intercostal spaces, and coxal tuberosity (13), are not helpful in chelonians because their body is protected by a rigid shell. Radiographic anatomic landmarks could help the interpretation of x-ray-film images of sea turtles and provide better determination of the diagnosis when other imaging modalities are not available.

The purpose of this investigation was to provide the normal cervical and coelomic radiographic appearance of the loggerhead sea turtle, in the dorsoventral view, as well as other useful landmarks, to allow for the correlation of shell scutes with internal anatomic structures.

Servei d'Ecopatologia de Fauna Salvatge (Valente, Cuenca, Lavín, Marco) and Departament de Medicina i Cirurgía Animals (Franch), Facultat de Veterinària, Universitat Autònoma de Barcelona, 08193 — Bellaterra, Barcelona, Spain; Centre de Recuperació d'Animals Marins, Camí Ral 239, 08330 — Premià de Mar, Barcelona, Spain (Parga).

Address all correspondence and reprint requests to Dr. Ana Luisa Valente; telephone: +34 93 581 19 23; fax: +34 93 581 20 06; e-mail: schifinoval@hotmail.com

Received November 9, 2005. Accepted March 6, 2006.

Materials and methods

Dorsoventral radiographs were taken of the neck and body of 15 juvenile and 15 subadult loggerhead sea turtles; 17 were alive and 13 dead. All had been accidentally caught in pelagic longline sets and fishing nets along the northwestern Mediterranean coast (40°31′ to 42°26′ north and 0°32′ to 3°10′ east). Juvenile turtles were considered to be those with a minimum straight carapace length (SCLmin) of 21 to 40 cm and subadults those with an SCLmin of 41 to 65 cm (14). Live turtles were temporally housed in the rehabilitation facilities of the Rescue Centre for Marine Animals (CRAM), Premià de Mar, Barcelona, Spain. Only clinically normal animals were included in the study.

No sedation was necessary for the examination. The animals were manually restrained, blindfolded, and positioned in ventral recumbency. At least 2 dorsoventral radiographs were taken of each turtle. Analog radiography was performed in 14 animals and digital radiography in the other 16. Tabletop images were taken with a Rotanode x-ray tube (model E7239; Toshiba Electron Tubes and Devices Company, Tokyo, Japan) at a focal distance of 68 cm. Analog radiography was performed with medical x-ray films used for mammography (UM-MA hc, 24 × 30 cm) and a Fuji AD-MA screen (UM MAMMO fine) and with Super HR-GB films 30 × 40 cm and rare-earth intensifying screens (Fuji ECD 30 × 40 cm), all from Fuji Photo Film Company, Tokyo, Japan. The radiographs were digitized on a flatbed scanner at a minimum resolution of 300 dots per inch. Digital radiography was performed with a digital flat-panel detector system (Regius cassette 14 × 17, Konica Minolta, Tokyo, Japan) and a Regius CR reader (model 170). All images were analyzed with Adobe Photoshop, version 5.5 (Adobe Systems, San Jose, California, USA); normal and inverted (negative) images were compared.

To correlate the external scutes with internal structures, we painted the union lines among the carapace scutes of 6 dead turtles with a radio-opaque product (anticorrosive paint with red lead oxide) before the radiographs were taken. Additionally, 3 dead turtles were injected with a solution of barium sulfate (Bario-dif Suspension, Rovi SA, Madrid, Spain) via the femoral vein to show the position of the kidneys. To visualize the jugular venous sinus and the large-intestine position, 2 other dead turtles were injected with the same contrast agent via the jugular vein and the cloaca, respectively. The anatomic terminology applied corresponds to that of the *Nomina Anatomica Veterinaria*. However, specific terminology for turtles (15) and sea turtles (16) was also applied.

Results

In the cervical region of the vertebral column, only the first 3 vertebrae were clearly imaged. The 4th cervical vertebra was partially seen because it is just below the cranial edge of the carapace (Figure 1). The contour of the 5th, 6th, and 7th cervical vertebrae could not be visualized. Although superimposed, the contour of the vertebral arches of these vertebrae (Figure 2B) could be identified in the juvenile turtles. The 10 dorsal vertebrae that form the carapace were visible, with a slim body, slightly broader in the extremities because the articular surface opposes the head of the ribs (Figure 3B). The vertebral bodies were seen to be elongated from the 2nd to the 6th dorsal vertebrae. The body contour of the 7th and 8th dorsal vertebrae was not clearly visible. In the costovertebral joints, from the 4th to the 10th dorsal vertebrae, each rib head was seen to be slightly caudal to the junction of 2 vertebral bodies (Figure 2A). The intervertebral space was visualized as a very fine and discrete radiolucent line, and the joint between the distal end of the ribs and the peripheral bones was clearly visible when mammographic film or digital radiography was used (Figure 3B). The 1st pair of ribs was seen to be very close to the 2nd pair, and the ribs were slimmer (Figure 3B). The 9th and 10th pairs of ribs were inconspicuous but seen caudal to an imaginary line transversely crossing the acetabulum. The 9th rib was seen to be short and caudally curved and the 10th rib shorter, pointed, and floating (Figure 4). The sutures between the pleural bones were easily identified on plain films as transverse radiolucent lines in the middle of the intercostal spaces (Figure 3). In 2 small juvenile turtles this suture was widely open. The fontanelles, the intercostal spaces not ossified in the distal third of the ribs, were

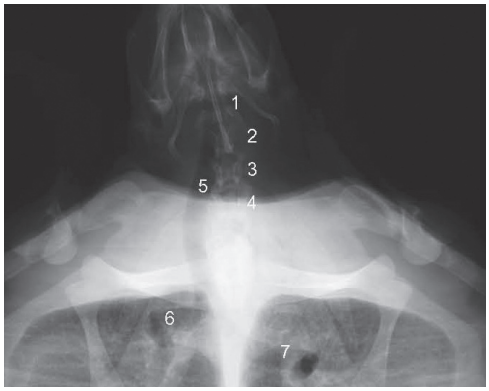

Figure 1. Dorsoventral radiographic view of the cranial end of a subadult loggerhead sea turtle. 1 — atlas; 2 — axis; 3 — 3rd cervical vertebra; 4 — 4th cervical vertebra; 5 — trachea; 6 — left bronchus; 7 — right bronchus.

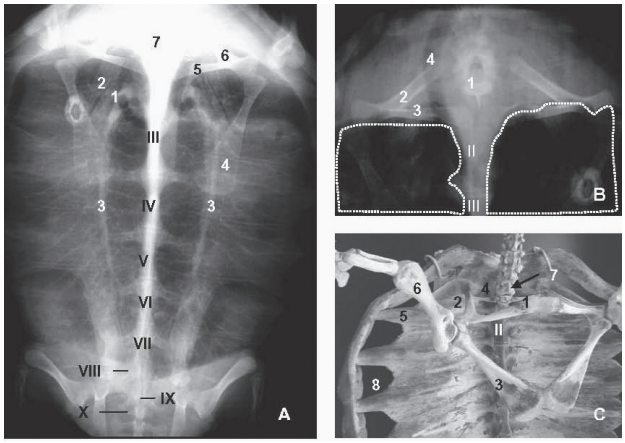

Figure 2. Dorsoventral radiographic views of subadult loggerhead sea turtles (A and B) and a ventral view of an adult loggerhead sea turtle's skeleton. Roman numerals indicate the respective dorsal vertebrae. A: 1 — bronchus; 2 — epiplastron; 3 — pulmonary blood vessels; 4 — coracoid bone; 5 — scapula; 6 — acromion; 7 — area of high radiodensity because of superimposition of osseous structures. B: 1 — cervical vertebral arches (superimposed); 2 — acromion; 3 — scapula; 4 — trachea. The cranial border of the pulmonary fields is delineated. C: 1 — scapula; 2 — acromion; 3 — coracoid bone; 4 — 1st pair of ribs; 5 — 2nd pair of ribs; 6 — humerus; 7 — 12th cervical vertebra; 8 — fontanelle.

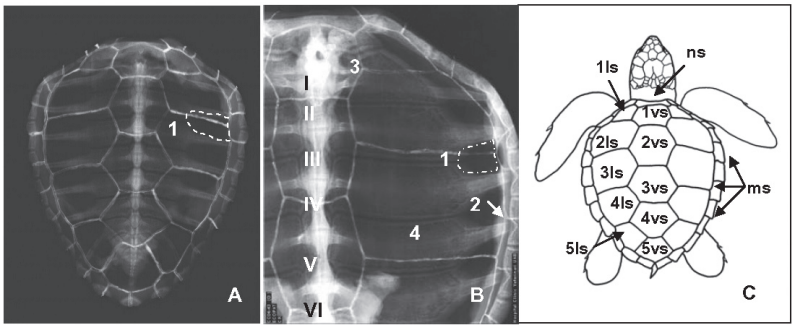

Figure 3. Digital dorsoventral radiographic views of the carapace of a juvenile loggerhead sea turtle of minimum straight carapace length (SCLmin) 23 cm (A) and a subadult of SCLmin 56 cm (B). Schematic drawing indicates the external scutes. A: 1 — widely opened fontanelle. B: 1 — partially ossified fontanelle; 2 — joint between rib and peripheral bone; 3 — 1st pair of ribs; 4 — sutures between the pleural bones. Roman numerals indicate the respective dorsal vertebrae. C: ls — lateral scute; ns — nuchal scute; vs — vertebral scute; ms — marginal scutes.

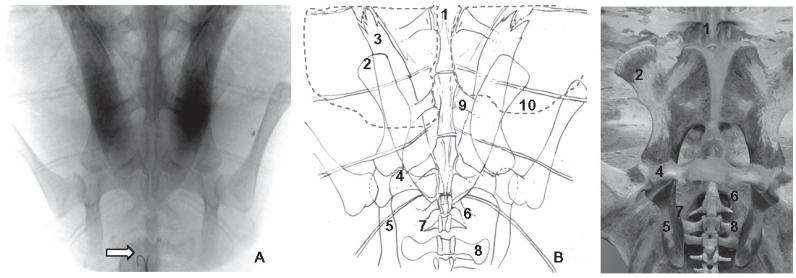

Figure 4. Negative image of the dorsoventral radiographic view of the pelvis of a subadult loggerhead sea turtle (A) and its interpreted drawing (B) and the ventral view of a skeletal pelvis (C). A: arrow indicates a fishhook in the rectum. B and C: 1 — 6th dorsal vertebra; 2 — lateral pubic process; 3 — xiphiplastron; 4 — ischium; 5 — ilium; 6 — 9th pair of ribs; 7 — 10th pair of ribs; 8 — transverse process of the 1st sacral vertebra; 9 — 7th pair of ribs; 10 — caudal border of the right pulmonary field.

extensively opened in all the turtles, but partial ossification was visible in 1 large subadult turtle (SCLmin 61 cm) (Figure 3).

The painted outline of the scutes was clearly visible in the radiographs. The images showed that the external keratinized scutes did not coincide with the pleural and neural bones (Figure 3). Each of the 5 vertebral scutes except the first and last (which are more caudal) completely covered 1 dorsal vertebra and half of the body of the preceding and following vertebrae, and each lateral scute covered 2 pairs of ribs (Figure 3). A difference in the ratio of length and width of the vertebral scutes was observed between the juvenile and subadult turtles, the scutes being wider than longer in the former (Figure 3). The relationship between the vertebral and lateral scutes and the osseous structure of the axial skeleton was constant and proportional in all of the turtles studied, independent of their size. The 3 sacral vertebrae were observed just below the 5th vertebral scute. Their bodies were shorter than those of the last dorsal vertebrae and showed a spatula-shaped transverse process articulating with the ilium (Figures 4 and 5). These vertebrae were not clearly visible in the juvenile turtles. Caudal vertebrae were variable in number.

The pectoral girdle was easily recognized in all films. It is formed by a union of 3 bony structures: scapula, acromion, and coracoid bone. These structures are jointed, forming about a 90° angle (Figure 2C). The acromion was seen to be completely ossified to the scapula, forming a single bone, and was identified as the most cranial of the 3 bones, followed caudally by the scapula (Figure 2B), which articulates with the carapace near the 1st dorsal vertebra. The Y-shaped structure thus formed is positioned horizontally on each side of the axial skeleton, just below the 1st vertebral scute, where the superimposition of the image of the cervical vertebrae forms an undefined central radio-opaque area (Figure 2A). The coracoid bone, caudal to the shoulder joint, has a flatter and wider shape at its caudal end (Figure 2). In all the turtles a radiolucent line could be seen at the union of the coracoid bone with the scapula.

The pubis and ischium form the ventrally positioned part of the pelvis, which was not clearly visible in the radiographs taken. Only the lateral pubic process and the articular end of the pubis could be clearly identified (Figure 4). The ischium was identified as an osseous bridge joining the acetabulum side to side. The image of this bone was usually superimposed by the silhouette of the 8th dorsal vertebra (Figure 4). The ilium was seen to be oriented dorsoventrally, articulating with the sacral vertebrae, which were easily recognized, as were the articular surfaces of the acetabular cavity (Figure 4).

The joint between the epiplastron and the hyoplastron was seen in the 1st third of the turtle's body as an oblique radiolucent line crossing the coracoid–acromion angle (Figure 6). The entoplastron could not be recognized owing to the great superimposition of the last cervical vertebrae. The suture between the hyoplastron and the hypoplastron was visible at the level of the 5th pair of ribs (5th dorsal

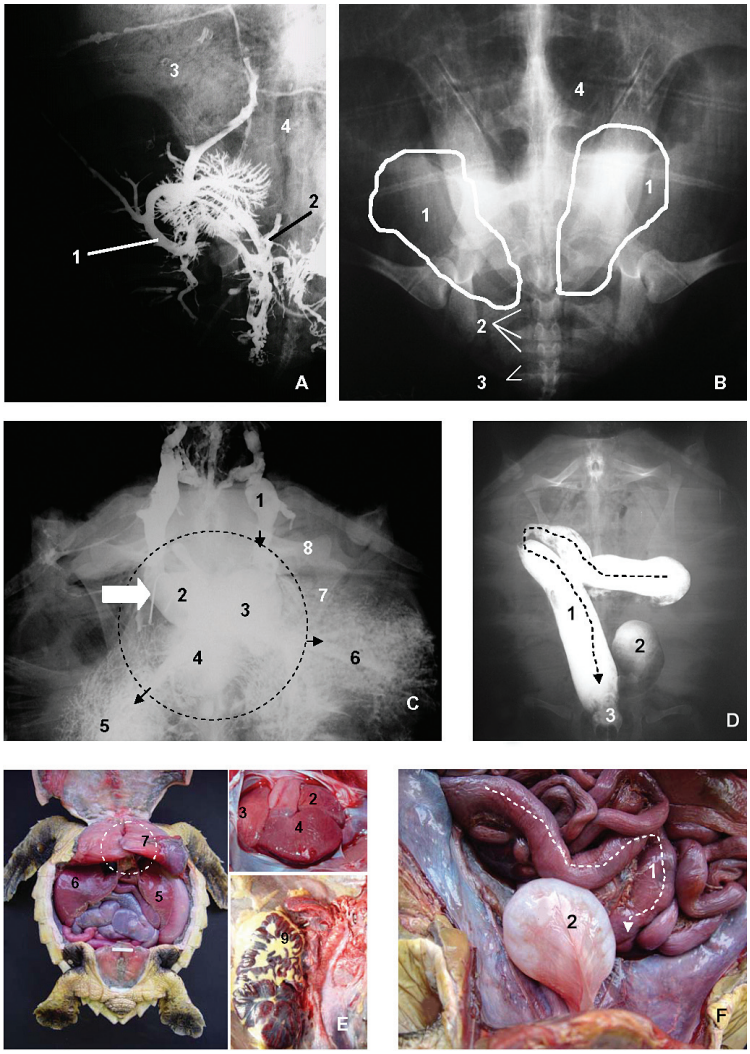

Figure 5. Dorsoventral radiographic views (A to D) and anatomic dissections (E and F) of subadult loggerhead sea turtles. A: renal vasculature injected with contrast agent; 1 — iliac vein; 2 — circumflex iliac vein; 3 — 4th costal scute; 4 — 4th vertebral scute. B: 1 — kidney positions; 2 — sacral vertebrae; 3 — caudal vertebrae; 4 — right pulmonary field. C: dorsoventral view of the cranial half of a dead juvenile loggerhead sea turtle injected with contrast agent; the heart position is delineated; 1 — sinus of the jugular vein; 2 — left atrium; 3 — right atrium; 4 — ventricle; 5 — left hepatic lobe; 6 — right hepatic lobe; 7 — scapula; 8 — coracoid. Small arrows indicate the jugular vein and the hepatic veins. White arrow indicates a fishhook. D and F: 1 — descending colon (enlarged in D by contrast injection); 2 — urinary bladder; 3 — cloacae. E: ventral view of a dissected turtle: 2 to 7 — same structures as shown in C; 9 — kidney.

vertebra) (Figure 6). The xiphiplastron images were superimposed with the images of the pubic bones, which produced some image distraction (Figure 6).

The position of the heart was recognized in relation to the skeleton and the sinus of the jugular vein in the dead animals injected with barium solution (Figure 5C and 5E). The heart was between the 1st to 3rd intercostal spaces, in the triangular area delineated by the coracoid bone and scapula (Figure 5C), and thus at the level of the 2nd vertebral scute. The trachea was easily identified on the left side of the cervical column (Figure 1), and its bifurcation to form the 2 long and extrapulmonary bronchi was visible at the level of the 2nd dorsal vertebra (Figure 2). The entrance of the right and left bronchi into the lungs was identified as 2 circular radiolucent areas at the level of the 1st dorsal vertebra (Figures 1 and 2). The pulmonary fields were very clearly imaged in all 17 live turtles and extended from the 1st to the 8th dorsal vertebrae. Although 9 of the turtles had symmetric lung fields, slight asymmetry between the right and left fields was observed in 8 turtles (Figures 2A and 5B). The pulmonary vasculature was very obvious, and the large pulmonary artery and vein were seen superimposed. They extended longitudinally in each lung (Figure 2A), and the collateral vasculature was frequently identified.

Visceral coelomic structural detail was often poor, and, in general, the clinically important organs, such as stomach, intestines, liver, and kidneys, were not imaged. Radio-opaque contents such as mollusk shells and fishhooks (Figure 4A), and even ingested coarse sand,

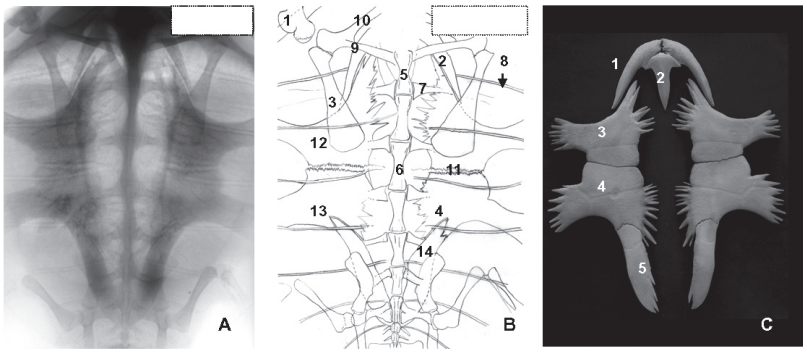

Figure 6. Negative image of the dorsoventral radiographic view of the whole body of a loggerhead sea turtle (A) and its interpreted drawing (B) and a ventral view of the plastron bones (C). B: 1 — humerus; 2 — epiplastron; 3 — coracoid bone; 4 — suture between the hypoplastron and the xiphiplastron; 5 — 2nd dorsal vertebra; 6 — 4th dorsal vertebra; 7 — 3rd pair of ribs; 8 — suture between the pleural bones; 9 — scapula; 10 — acromion; 11 — suture between the hyoplastron and the hypoplastron; 12 — hyoplastron; 13 — hypoplastron; 14 — xiphiplastron. C: 1 — epiplastron; 2 — endoplastron; 3 — hyoplastron; 4 — hypoplastron; 5 — xiphiplastron.

were identified in the gastrointestinal tract of some clinically healthy turtles. Intestinal loops were recognized when filled by radio-opaque digestive content or luminal gas and were interpreted as normal. Radio-opaque contrast material injected via the cloaca in dead turtles allowed visualization of the caudal part of the large intestine and identification of the urinary bladder (Figures 5D and 5F).

The position of the kidneys was recognized only once their vasculature was filled with contrast agent (Figures 5A, 5B, and 5E). They were seen at the level of the 8th to 10th dorsal vertebrae, below the 4th vertebral scute and the 4th and 5th left and right lateral scutes.

Discussion

Radiography is a useful tool to diagnose diseases of the skeleton and alimentary disorders in reptiles (1). In chelonians, pulmonary diseases, nutritional osteofibrosis, fractures, dystocia, and alimentary obstructions are the most important indications for radiographic diagnosis (7). According to previous studies (3), dorsoventral radiographs are the most suitable views for evaluating major organ systems in chelonians. In this study, we have verified that with careful adjustments to the kilovoltage potential (kVp) and the milliamperage-seconds (mAs) it is possible to gain much valuable information from dorsoventral radiography in loggerhead sea turtles. Digital radiography improves contrast and makes these adjustments easier. In reptiles, images produced with the matched mammography film–screen combination have greater resolution and better detail than standard tabletop radiographs (4). The film–screen combination was not as useful in evaluating coelomic structures in loggerhead sea turtles as in other chelonian species owing to the small screen size and the great thickness of the turtle's body, as well as the high radiodensity of their osseous structures, which made it necessary to increase the kVp to obtain more penetrability, thus causing loss of contrast. In addition to the use of digital images, the adjustment to a negative view was a reliable way of having ossified structures stand out, which made the recognition of the skeleton easier.

As a result of the variability of radiodensity in the different tissues and parts of the body, it was necessary to increase the kVp in the cranial third of the carapace and decrease it in the caudal third. Generally, individual identification of the vertebral bodies in the chelonians was difficult because of the superimposition of their images with those of the neural bones of the carapace. In addition, the intervertebral spaces (intercentral joints), easily recognized on radiographs in mammalian (17) and other reptilian species, is seen in chelonians as a very narrow and discrete radiolucent line that cannot be clearly imaged if a suitable kVp is not used. In large turtles, we recommend taking radiographs by sectors and using anatomic landmarks that allow spatial location of the affected areas, minor distortion or magnification, and better set-up of the adjustments.

In dorsoventral screening of the turtle's body, one must take into account the distortion caused by the natural curvatures of the body, which are seen at 2 points in the vertebral column: the S-shaped curvature of the cervical region, which causes the superimposition of images of the 5th and 6th cervical vertebrae, and the ventral flexion of the vertebral column from the 6th to the 10th dorsal vertebrae, which produces distortion in the length and partial superimposition of images of the vertebral bodies.

Knowledge of the relationship between the external scutes (used as external landmarks) and the vertebral column allows for efficient radiographic evaluation of traumatic injuries of the carapace, mainly those caused by propellers that affect the vertebral column and cause neurologic symptoms, once the injured vertebrae have been accurately identified (18).

Other anatomic landmarks useful in interpreting radiographs of the loggerhead sea turtle include the bronchi, coracoid bones, caudal border of the pulmonary fields, and acetabulum. Unlike that in most species of chelonians (1), the pulmonary field in healthy loggerhead sea turtles was easily identified in the dorsoventral view. Although in chelonian medicine, lateral and craniocaudal views are the most informative in assessing pulmonary disease (7,19), these views are often limited in the loggerhead sea turtle owing to the large size and high radiodensity of the body. Dorsoventral views are of reliable value because they allow clear recognition of any alteration in form, size, or appearance of the pulmonary field.

The morphologic differences observed in the turtle's pelvis (16) as compared with a mammalian pelvis (20) should be taken into account to avoid misinterpretation in identifying the pelvic bones. In the loggerhead sea turtle, the pubis is visible cranial to the acetabulum, in a position analogous to that of the mammalian ilium, the ischium is visible in a position analogous to that of the mammalian pubis, and the ilium is visible caudal to the acetabulum, in a position analogous to that of the mammalian ischium.

In conclusion, we have presented the standard radiologic appearance of the cervical and coelomic structures of the loggerhead sea turtle to help clinicians in evaluating radiographic abnormalities.

Acknowledgments

We thank Dr. Jaume Martorell, Departament de Medicina i Cirurgía Animals, Facultat de Veterinària, Universitat Autònoma de Barcelona, for his help with the radiography. We also thank CRAM volunteers and veterinary students Meritxell Clavell, Carolina Garcia, Loana Fraga, and Olga Nicolas for their help with the turtle procedures. Thanks also go to Drs. Manel López Bejar and Carlos López Plana, Departament de Sanitat i Anatomia Animals, Facultat de Veterinària, Universitat Autònoma de Barcelona, for generously supplying the turtle skeleton. We also thank the anonymous peer reviewers.

References

1. Rübel A, Kuoni W. Radiology and imaging. In: Frye FL, ed. Biomedical and Surgical Aspects of Captive Reptile Husbandry. 2nd ed. Melbourne, Florida: Krieger Publishing, 1991:185–208.
2. Jackson OF, Sainsbury AW. Radiological and related investigations. In: Beynon PH, ed. Manual of Reptiles. Quedgeley, England: British Small Animal Veterinary Association, 1992:63–72.
3. Silverman S, Janssen D. Diagnostic imaging. In: Mader DR, ed. Reptile Medicine and Surgery. Philadelphia, Pennsylvania: W.B. Saunders, 1996:258–264.
4. DeShaw B, Schoenfeld A, Cook RA, Haramati N. Imaging of reptiles: a comparison study of various radiographic techniques. J Zoo Wildl Med 1996;27:364–370.
5. Meyer J. Gastrografin as a gastrointestinal contrast agent in the Greek tortoise (*Testudo hermanni*). J Zoo Wildl Med 1998;29: 183–189.
6. Gaudron C, Lignereux Y, Ducos de Lahitte J. Imagerie médicale appliquée à l'anatomie clinique des chéloniens en consultation. Proc Int Meet *Testudo* Genus 2001:161–182.
7. Wilkinson R, Hernandez-Divers S, Lafortune M, Calvert I, Gumpenberger M, McArthur S. Diagnostic imaging. In: McArthur S, Wilkinson R, Meyer J, eds. Medicine and Surgery of Tortoises and Turtles. Victoria, Australia: Blackwell Publishing, 2004:187–238.
8. Mader D. Radiographic anatomy. In: Mader DR, ed. Reptile Medicine and Surgery. Philadelphia, Pennsylvania: W.B. Saunders, 1996:485–489.
9. Pont SG, Alegre FN. Work of the Foundation for the Conservation and Recovery of Marine Life. Marine Turtle Newsl 2000;87: 5–7.
10. McArthur S. Problem-solving approach to conditions of marine turtles. In: McArthur S, Wilkinson R, Meyer J, eds. Medicine and Surgery of Tortoises and Turtles. Victoria, Australia: Blackwell Publishing, 2004:301–307.
11. Maudgil DD, Free SL, Sisodiya SM, Lemieu L, Woermann FG, Fish DR. Identifying homologous anatomical landmarks on reconstructed magnetic resonance images of the human cerebral cortical surface. J Anat 1998;193:559–571.
12. Bookstein FL. Morphometric Tools for Landmark Data: Geometry and Biology. New York, Cambridge University Press, 1991.
13. Radostits OM, Mayhew IG, Houston DM. Examen y diagnóstico clínico en veterinaria. 2nd ed. Madrid, Spain: Ediciones Harcourt, SA, 2002:409–467.
14. Dodd CK Jr. Synopsis of the Biological Data on the Loggerhead Sea Turtle *Caretta caretta* (Linnaeus 1758). US Fish and Wildlife Service Biological Report 1988:88(14).
15. Holz P, Barker IK, Crawshaw GJ, Dobson H. The anatomy and perfusion of the renal portal system in the red-eared slider (*Trachemys scripta elegans*). J Zoo Wildl Med 1997;28:378–385.
16. Wyneken J. The Anatomy of Sea Turtles. US Department of Commerce NOAA Technical Memorandum NMFS-SEFSC 2001;470:43–58.
17. Smallwood JE, Spaulding KA. Radiographic anatomy of the dog and horse. In: Thrall DE, ed. Textbook of Veterinary Diagnostic Radiology. 2nd ed. Philadelphia, Pennsylvania: W.B. Saunders, 1994:556–602.
18. Parga ML, Valente AL, Zamora MA, et al. Carapace trauma associated with hind limb paralysis in a loggerhead sea turtle (*Caretta caretta*). Proc Spring Meet Br Vet Zool Soc 2005:41.
19. Hernandez-Divers S, Hernandez-Divers S. Diagnostic imaging of reptiles. In Practice 2001;23:370–391.
20. Newton CD. Fractures of the pelvis. In: Newton CD, Nunamaker MJB, eds. Textbook of Small Animal Orthopaedics. Philadelphia, Pennsylvania: J.B. Lippincott, 1985.